PROCEEDINGS OF SCIENCE

Quark-hadron deconfinement for hot, dense and rotating matter under magnetic field

Gaurav Mukherjee,[a,b,*] **D.Dutta**[a,b] **and D.K.Mishra**[a,b]

[a] *Bhabha Atomic Research Center, Mumbai 400085, India*

[b] *Homi Bhabha National Institute, Anushaktinagar, Mumbai 400094, India*

E-mail: phy.res.gaurav.m@gmail.com

The early universe and ultra-relativistic heavy-ion collisions are arenas where QCD matter exists under extreme conditions. Considering the overlap in a generic non-central high-energy nucleus-nucleus collision, the created fireball of quark-gluon plasma (QGP) can sustain strong vorticity due to the finite impact parameter arising from the geometry of the collision and the resultant deposition of angular momentum. This QGP droplet can be embedded in strong magnetic fields that are sourced by the spectator protons of the incident nuclei and likely sustained by the the conductivity and swirling charges in the fluid medium. Such a physical system inspires a suitable extension of the conventional T–μ_B QCD phase diagram. We augment the temperature, T, and baryon chemical potential, μ_B, axes with one for external magnetic field, B, and another for angular velocity, ω. To achieve this, we identify the confinement-deconfinement transition region of the phase space. This is implemented via two independent routes, one from a rapid rise in scaled entropy density and another dealing with a dip in the squared speed of sound, both within the framework of a modified statistical hadronization model. We find that this approach yields an estimate of the deconfinement temperature $T_C(\mu_B,\ \omega,\ eB)$ that is found to decrease with increasing μ_B, ω and eB. The most prominent drop (by nearly 40 to 50 MeV) in T_C occurs when all the three quasi-control (dependent on collision energy, centrality class, etc.) parameters are tuned to values that are achievable in present and upcoming heavy-ion colliders. We also propose some potentially important magneto-rotational consequences on quark-hadron phenomenology such as a reinterpretation of chemical freeze-out data from peripheral collisions in the service of measurements of the fireball's magnetic field (magnetometer) and vorticity (anemometer).

XVIth Quark Confinement and the Hadron Spectrum Conference
19-24 August, 2024
Cairns, Queensland, Australia

*Speaker

PoS(QCHSC24)172

1. Motivation and introduction

QCD matter under extreme conditions prevailed in the microsecond-old universe and is created in ultra-relativistic heavy-ion collisions. In a typical non-central or peripheral high-energy nucleus-nucleus collision, a QGP fireball forms and this can sustain swirling motion quantified by vorticity (experiments [1] indicate $\omega \approx (9 \pm 1) \times 10^{21} s^{-1} \sim 0.006$ GeV, higher theoretical estimates [2] yield $\omega \sim 0.1$ fm$^{-1} \sim 0.02$ GeV) due to the finite impact parameter. The droplet may also be embedded in very powerful magnetic fields ($eB \sim 0.12$ GeV^2) sourced at the earliest instants by the spectator protons of the colliding nuclei [3]. The magnetic field is likely sustained and reinforced as a result of the conductivity and swirling charges of the QGP medium [4]. This system, around 10 fm across and living for $\sim 10^{-23}$ s, is record-setting in several respects, such as being the hottest, densest, most vortical fluid and embedded in the strongest known magnetic fields.

This motivates a suitable extension of the conventional (T–μ_B) planar phase diagram for QCD matter by augmenting it into a multi-dimensional domain spanned by temperature (T), baryon chemical potential (μ_B), external magnetic field (eB) and angular velocity (ω). Certain effects of finite μ_B, ω, and eB, have been studied separately or in pairs in the literature before [5–8]. We fully explore their interplay and combined impact here. For a more detailed account, see our paper [9].

We shall adopt a modified hadron resonance gas (HRG) model. Our investigation of the deconfinement (crossover) zone in the augmented QCD phase diagram should be relevant for present (RHIC, LHC) and upcoming (NICA, FAIR) colliders. Two independent methods will be used to estimate the pseudocritical temperature. These are mutually corroborated. We conclude with some interesting implications of our findings and an outlook for future research.

2. Model formalism

We study a relativistic quantum ideal gas within a cylinder of radius R, which rotates globally and is immersed in a parallel magnetic field. In such a system composed of both charged as well as neutral particles the former couple with the background magnetic field while the latter do not, to a first approximation. To discuss just the magnetic coupling of a charged particle of charge Q, we need Landau levels, $\varepsilon = \sqrt{p_z^2 + p_\perp^2 + m^2} = \sqrt{p_z^2 + |QB|(2n + 1 - 2s_z) + m^2}$, with $n = 0, 1, 2, \ldots$. They appear in a finite-sized system with degeneracy $N = \frac{|QB|S}{2\pi}$ where $S \sim R^2$ ($S = \pi R^2$, for our geometry) is the transverse area. Landau quantization dominates as long as $N \gg 1$ or equivalently $\frac{1}{\sqrt{|QB|}} \ll R$. In other words, the magnetic length ($\frac{1}{\sqrt{|QB|}} \equiv l_B$) which is the characteristic length scale for the cyclotron orbits, should be sufficiently smaller than the system size ($R = l_{\text{system}}$). The boundary or finite size becomes important when $l_{\text{system}} \lesssim l_B$ and the degenerate Landau quantized spectra no longer apply.

Since we use the Landau quantized levels we can investigate magnetic fields that are not too weak. The introduction of rigid rotation means the system must have a finite transverse size so that all speeds are below the vacuum speed of light, $c = 1$. This causality bound and Landau quantization together imply

$$1/\sqrt{|QB|} \ll R \leqslant 1/\omega. \tag{1}$$

The free energy density of the entire system in our model is the sum of the contributions from all the non-interacting hadrons and resonances in the HRG model. Our sought modifications to the standard HRG model, adapted to the scenario incorporating a uniform external magnetic field as well as a parallel rigid rotation have been deduced [6, 9, 10]. The free energy density for charged baryons and mesons is expressed as

$$f_{i,c}^{b/m} = \mp\frac{T}{\pi R^2}\int\frac{dp_z}{2\pi}\sum_{n=0}^{\infty}\sum_{l=-n}^{N-n}\sum_{s_z=-s}^{s}\ln(1\pm e^{-\frac{E_{i,c}}{T}}), \tag{2}$$

while that of the neutral ones [7, 9] is given by

$$f_{i,n}^{b/m} = \mp\frac{T}{8\pi^2}\int dp_r^2\int dp_z\sum_{l=-\infty}^{\infty}\sum_{\nu=l}^{l+2S_i}J_\nu^2(p_r r)\times\ln(1\pm e^{-\frac{E_{i,n}}{T}}), \tag{3}$$

where the dispersion relations provide the required energy spectra given by the rotation-modified levels (Landau levels for non-zero magnetic field):

$$E_{i,c} = \sqrt{p_z^2+m_i^2+|e_iB|(2n-2s_z+1)} \quad +\frac{e_i}{|e_i|}\omega(l+s_z)-\mu_i, \tag{4}$$

$$E_{i,n} = \sqrt{p_r^2+p_z^2+m_i^2}-(l+S_i)\omega-\mu_i. \tag{5}$$

Here e_i, S_i and m_i are the charge, spin and mass of the i^{th} hadron and the subscripts c and n refer to charged particles and neutral particles respectively. The chemical potential $\mu = Q_B\mu_B + Q_e\mu_e + Q_S\mu_S$ reflects the baryonic, electric charge and strangeness components. The upper (lower) signs correspond to the baryons (mesons) as denoted by the superscript b (m). The rotation is seen to alter the energy dispersion by an offset that effectively acts as a 'rotational' chemical potential by analogy [10]. We have taken fixed values of $r = 3$ GeV^{-1} and $R = 12.5$ GeV^{-1} (or $R = 2.5$ fm, $\sim$ typical system radius for peripheral collisions).

For the system we are dealing with, the free energy density reads $f = \epsilon - Ts - \mu_B n_B - \omega j - Bm_B = -p$, where pressure p, energy density ϵ, entropy density s, number density n_B, magnetization m_B and total angular momentum j are the relevant observables. All the observables here satisfy simple differential relations, $s = -\frac{\partial f}{\partial T}$, $n_B = -\frac{\partial f}{\partial \mu_B}$, $j = -\frac{\partial f}{\partial \omega}$, $m_B = -\frac{\partial f}{\partial B}$. The squared speed of sound is defined as $c_s^2 = \frac{\partial p}{\partial \epsilon}|_{(\mu_B,\omega,eB)} = [\frac{\partial p}{\partial T}|_{(\mu_B,\omega,eB)}]/[\frac{\partial \epsilon}{\partial T}|_{(\mu_B,\omega,eB)}]$ and here comes out to be

$$c_s^2 = \frac{s}{\left(T\frac{\partial s}{\partial T}+B\frac{\partial m_B}{\partial T}+\omega\frac{\partial j}{\partial T}+\mu_B\frac{\partial n_B}{\partial T}\right)\Big|_{(\mu_B,\omega,eB)}} \tag{6}$$

All hadrons, up to a mass of 1.5 GeV and excluding those having spin-3/2, listed in the particle data group list of particles contained in the package of THERMUS-V3.0 [12] have been included in our HRG model treatment. The ultraviolet mass cut-off is taken to reduce numerical cost and the exclusion of the spin-3/2 sector has been implemented due an instability in its theory [11].

3. An augmented phase diagram

Our strategy is to study characteristics that serve as proxies for the onset of deconfinement. We exploit an argument based on the Hagedorn limiting temperature concept [7, 13–16]. We compute

the entropy density numerically and impose the criteria $s/T^3 = 4 - 7$ to constrain the range within which the deconfinement transition occurs most rapidly. This leads to the deconfinement bands shown in Fig. 1 for the scenarios without ($eB = 0$) and with ($eB = 0.15$ GeV^2) magnetic field.

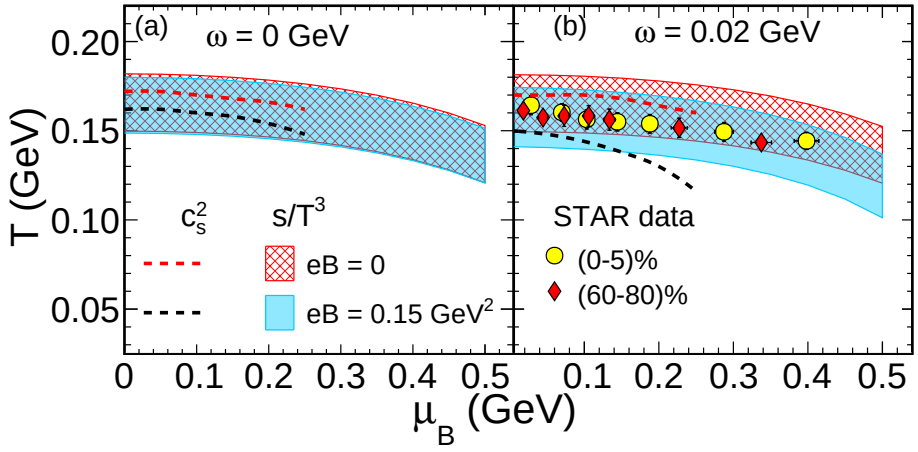

Figure 1: QCD phase diagrams, T vs. μ_B for $eB = 0$ (red band or curve) and $eB = 0.15$ GeV^2 (blue band or curve) and (a) for $\omega = 0$ GeV and (b) for $\omega = 0.02$ GeV. The deconfinement transition zones depicted as (i) bands constrained by $s/T^3 = 4$ (lower edge) and 7 (upper edge) , and (ii) curves obtained from the minima of c_s^2 vs. T.

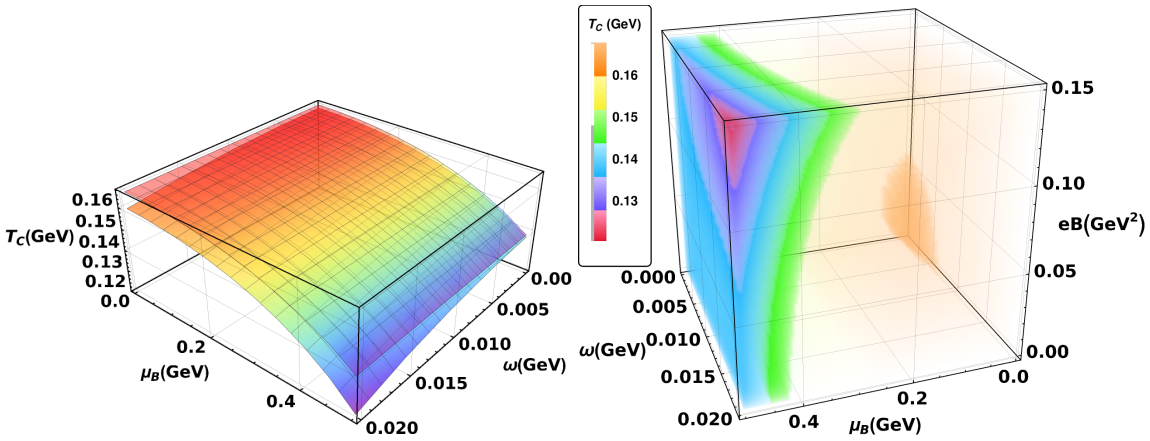

Figure 2: (Top) Deconfinement transition surfaces showing $T_C(\mu_B,\ \omega)$ for $eB = 0$ (upper surface) and $eB = 0.15$ GeV^2 (lower surface). (Bottom) Augmented phase diagram showing $T_C(\mu_B,\ \omega,\ eB)$ as a colour-coded density plot where the T_C-calibrated legend (left) provides reference for the different iso-T_C contour boundaries in the $\mu_B,\ \omega,\ eB$ space. Both plots obtained from rapid rise in entropy density at $s/T^3 = 5.5$.

We observe a successive lowering of the crossover band due to finite magnetic field as ω rise from 0 to 0.02 GeV ($\sim 3 \times 10^{22} s^{-1}$). The dip in T_C is amplified substantially, reaching a nadir nearing 0.1 GeV. At zero magnetic field the effect of rotation with ω rising from 0 to 0.02 GeV is only slight within the range considered here. However, the simultaneous imposition of an external magnetic field over and above the rotation leads to nearly the same drop in the deconfinement temperature at $\omega = 0.02$ GeV as that estimated at extremely large values of $\omega = 0.3$ GeV when there is no magnetic field present at all [7]. This suggests that although the latter (pure, $eB = 0$) rapid

rotation scenario might be too high for a typical HIC at deconfinement and freeze-out, a similar (in magnitude) effective lowering of T_C may nevertheless still apply if a strong enough $eB \sim 0.12$ GeV^2 accompanies the more modest but also more plausible $\omega \sim 0.02$ GeV, as we study here. As the QGP droplet produced in a HIC (particularly those with finite μ_B, ω and eB) evolves from its initial formation to hadronization, the pronounced lowering of T_C may lead to a longer lifetime for the deconfined phase.

In Fig. 1, we have also shown data points for chemical freeze-out [17] for two centrality classes, (0-5)% and (60-80)%. The analyses of peripheral collisions in such studies does not take into account ω and eB. After incorporating all quasi-control parameters (μ_B, ω and eB, all dependent on collision energy and impact parameter or centrality) for freeze-out calculations, instead of a just a $(T - \mu_B)$ curve serving as 'thermometer' and 'baryometer' we can possibly augment them with capabilities of 'magnetometer' and 'anemometer'. The degree of the relative influences of μ_B, ω and eB may be constrained from other simultaneous observables, for example measured polarization [1] to independently constrain ω, etc.

Figure 2 shows the surface plots (3-D QCD phase diagram) $T_C(\mu_B, \omega)$ for $eB = 0$ and $eB = 0.15$ GeV^2. An even more fine-grained data set is also exhibited in the (4-D QCD phase diagram) $T_C(\mu_B, \omega, eB)$ density plot in Fig. 2.

A dip in the squared speed of sound, c_s^2, reveals the softest point in the equation-of-state and signals a phase transition. Both methods lead to the conclusion that the drop in T_C is strongly enhanced at high μ_B, ω and eB.

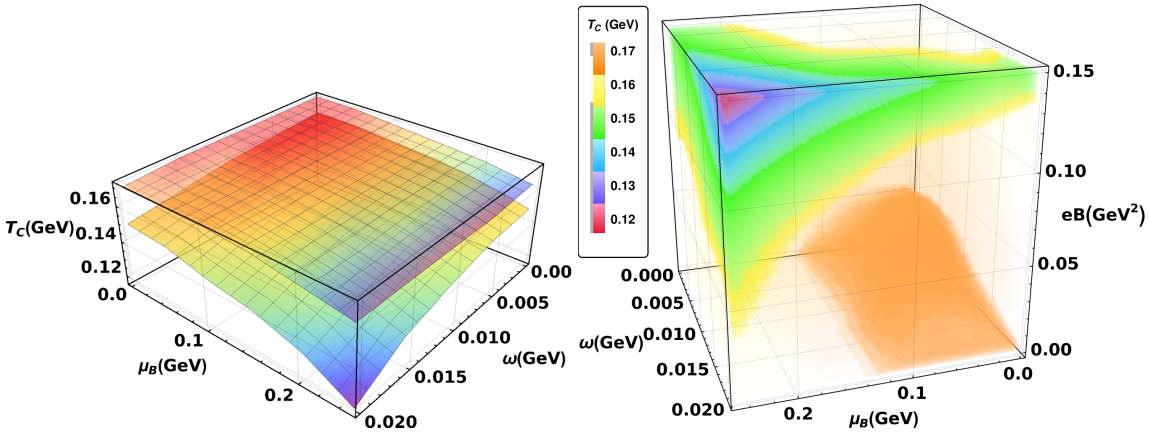

Figure 3: (Top) Deconfinement transition surfaces showing $T_C(\mu_B, \omega)$ for $eB = 0$ (upper surface) and $eB = 0.15$ GeV^2 (lower surface). (Bottom) Augmented phase diagrams showing $T_C(\mu_B, \omega, eB)$, analogous to Fig. 2. Both obtained from the minima of the squared speed of sound.

Figure 3 shows the T_C values obtained from the speed of sound analysis. These results are closely analogous to those shown in Fig. 2.

4. Discussion and conclusions

We painted a quantitative picture of the $T - \mu_B - \omega - eB$ space and focused on the quark-hadron crossover region. Thus, the QCD phase structure was expanded to accommodate two

new parameters, namely vorticity and magnetic field. To implement the mapping of this hitherto unexplored terrain in phase space, we built the required theoretical tools within the framework of the statistical hadronization model. We arrived at a consistent and robust prediction for the deconfinement temperature T_C as a function of μ_B, ω, and eB. To visualize the behavior of the transition, we plotted phase diagrams in 2D, 3D, and 4D.

We explained the possible strategies that could be adopted in order to apply this knowledge to trace out freeze-out curves (rather, surfaces or volumes) in the higher-dimensional phase space and probe HIC fireballs in the capacity of measurement tools akin to an anemometer and magnetometer. The fact that the model gives consistent and corroborating evidence with respect to the decreasing trend of the deconfinement temperature is a reason for confidence. This provides a certain perspective in the currently ongoing discussion within the quark matter and heavy-ion community.

Since *both* a global vorticity *and* an external magnetic field are probably present simultaneously in the fireball, they act together. When this is the case, the net effect is drastically stronger than any of the individual contributions or even a simple sum of the latter. In this sense, the combined effect or the '*whole is greater than the sum of its parts.*' This result is quite non-trivial and it is a consequence of the highly non-linear (QCD itself as well as magnetovorticity) nature of the problem. Given that lattice QCD and other complementary methods deal mostly in either a magnetic field only or rotation alone, it is to be seen whether our results are supported and further strengthened in subsequent research using these alternate methods and also whether particle yield and ratio data from non-central collisions corroborate the suggestive trend regarding the chemical freeze-out curves. If the results turn out to be valid, then one can make conclusive predictions about more observables that are anticipated to be affected substantially by both magnetic field and vorticity. Hopefully, the convoluted interactions involved can be disentangled in the near future to better elucidate the generalized magnetovortically augmented QCD phase structure. Starting from the T axis where μ_B, ω, and eB are all zero, if we can venture into the hinterland of this fascinating phase space, then we have the opportunity to pioneer uncharted territory and might even arrive at a critical point (or rather curve or surface) that legitimizes the quark-hadron duality in the supercritical crossover region as a true first-order phase transition. Whether it would become experimentally feasible to firmly plant a flag upon reaching the till-now hypothetical critical point is a possibility that may well be realized at RHIC, FAIR, or NICA in the near future.

The following key points serve as the takeaway of the present study:

- Global vorticity and external magnetic field should exist in tandem and influence the hot and baryon-rich fireball produced in any generic off-central heavy-ion collision.
- An augmented QCD phase diagram is desired and can serve as an embedding parameter space for the trajectories of the evolving system.
- The crossover part of this higher dimensional comprehensive phase space was mapped using the statistical hadronization model.
- Two distinct approaches that yield T_C, the pseudo-critical or deconfinement temperature, were applied to obtain the phase diagram and were found to agree on the general trend followed by the confinement-deconfinement crossover band or boundary.

- In one approach, we computed the squared speed of sound as a function of temperature and varied the various parameters independently to monitor the behavior of the non-monotonic part of the function, namely the minimum point. These dips were interpreted to indicate the onset of deconfinement and the observed trend showed that deconfinement happens at successively cooler and cooler temperatures with increasing μ_B, ω and eB. It was also noticed that the the dips grew deeper, i.e., the equation of state became softer for higher values of these independent variables.

- The other distinct approach of locating the region of rapid rise in thermodynamic observables such as the scaled entropy density yielded a parallel trend. These corroborating results support the robustness of the methods used and are suggestive of a potentially significant effect.

- The quark-hadron deconfinement temperature T_C, for a system under simultaneously finite μ_B, ω and eB, is observed to drop quite drastically, by nearly 40 to 50 MeV. This suggests that μ_B, ω and eB somehow act strongly cooperatively in lowering T_C and that too in a way that far exceeds any of their individual or even pairwise capacities. This suggests that confinement-deconfinement occurs at somewhat cooler temperatures in highly magnetized and globally vortical quark matter systems.

- The range of magnitudes for μ_B, ω and eB considered in the theoretical modeling here include the estimated values of these parameters that should be typical at heavy-ion facilities (presently running colliders like LHC, RHIC, and upcoming ones such as FAIR, NICA, JPARC-HI, HIAF, etc.).

- The above results were obtained under a fortuitous confluence of circumstances by which the fireball size, vorticity and magnetic field all concomitantly obey both the Landau quantization criterion and the causality condition.

- It was emphasized that the model could effectively serve as (hadrochemical freeze-out) probes or measurement tools. The estimation of the freeze-out temperature and baryon chemical potential that is used extensively by the application of the statistical hadronization model in standard form inspires us to extend the same method to measuring the global vorticity and magnetic field at freeze-out.

- By perfecting a suitable prescription that can be formulated in tandem with another independent observable (for example, global vorticity can be obtained from $\Lambda - \bar{\Lambda}$ polarization), we might be able to uniquely, precisely, and unambiguously constrain the values of μ_B, ω and eB. This is the basis of the suggestion behind using the model methods as not only a thermometer and baryometer but also as an anemometer and magnetometer. Before this can be achieved, however, and to accurately extract such important features of the HIC fireball, the model assumptions and approximations would likely need further refinement. This can be pursued as a future direction for research, to advance beyond the first step taken here. The ideal conditions of the 'toy' model can be replaced with more realistic considerations, if needed.

- Vorticity and net baryon density are larger when the collision energy is low and the magnetic field is also more enduring for such collisions. For non-central collisions, therefore, a net effect should be sourced by all these three variables. We expect that experimental signals should be able to support the performed analyses and obtained results.

References

[1] STAR Collab., *Global Λ hyperon polarization in nuclear collisions*, Nature 548, 62–65 (2017) (arXiv:1701.06657)

[2] Yin Jiang, Zi-Wei Lin, and Jinfeng Liao, *Rotating quark-gluon plasma in relativistic heavy-ion collisions*, Phys. Rev. C 94, 044910; Erratum Phys. Rev. C 95, 049904 (2017) (arXiv:1602.06580)

[3] Xu-Guang Huang, *Electromagnetic fields and anomalous transports in heavy-ion collisions—a pedagogical review*, Rep. Prog. Phys. 79 076302 (2016) (arXiv:1509.04073)

[4] Xingyu Guo, Jinfeng Liao and Enke Wang, *Spin Hydrodynamic Generation in the Charged Subatomic Swirl*, Scientific Reports volume 10 (2020) (arXiv:1904.04704)

[5] Kenji Fukushima and Yoshimasa Hidaka, *Magnetic Shift of the Chemical Freeze-out and Electric Charge Fluctuations*, Phys. Rev. Lett. 117, 102301 (2016) (arXiv:1605.01912)

[6] Yizhuang Liu and Ismail Zahed, *Pion Condensation by Rotation in a Magnetic Field*, Phys. Rev. Lett. 120, 032001 (2018) (arXiv:1711.08354)

[7] Yuki Fujimoto, Kenji Fukushima, and Yoshimasa Hidaka, *Deconfining phase boundary of rapidly rotating hot and dense matter and analysis of moment of inertia*, Physics Letters B Volume 816, 136184 (2021) (arXiv:2101.09173)

[8] Yin Jiang and Jinfeng Liao, *Pairing Phase Transitions of Matter under Rotation*, Phys. Rev. Lett. 117, 192302 (2016) (arXiv:1606.03808)

[9] Gaurav Mukherjee, D. Dutta, D.K. Mishra, *An augmented QCD phase portrait: Mapping quark-hadron deconfinement for hot, dense, rotating matter under magnetic field*, Physics Letters B 846, 138228 (2023) (arXiv:2304.12643)

[10] Hao-Lei Chen, K. Fukushima, Xu-Guang Huang, and K. Mameda, *Analogy between rotation and density for Dirac fermions in a magnetic field*, Phys. Rev. D 93, 104052 (2016) (arXiv:1512.08974)

[11] Endrődi, G., *QCD equation of state at nonzero magnetic fields in the Hadron Resonance Gas model*, J. High Energ. Phys. 2013, 23 (2013) (arXiv:1301.1307)

[12] S. Wheaton, J. Cleymans, M. Hauer, *THERMUS—A thermal model package for ROOT*, Computer Physics Communications, Volume 180, Issue 1, 2009, https://doi.org/10.1016/j.cpc.2008.08.001

[13] R. Hagedorn, *Statistical thermodynamics of strong interactions at high-energies*, Nuovo Cim.Suppl. 3 (1965) 147-186, https://cds.cern.ch/record/346206

[14] Johann Rafelski, *Melting Hadrons, Boiling Quarks - From Hagedorn Temperature to Ultra-Relativistic Heavy-Ion Collisions at CERN*, https://doi.org/10.1007/978-3-319-17545-4 (arXiv:1508.03260)

[15] N. Cabibbo, G. Parisi, *Exponential Hadronic Spectrum and Quark Liberation*, Physics Letters B, Volume 59, Issue 1, 13 October 1975, https://doi.org/10.1016/0370-2693(75)90158-6

[16] Kenji Fukushima, *Phase diagram of hot and dense QCD constrained by the Statistical Model*, Physics Letters B, Volume 695, Issues 1–4, 10 January 2011, Pages 387-391, https://doi.org/10.1016/j.physletb.2010.11.040 (arXiv:1006.2596)

[17] STAR Collaboration, *Global polarization and parity violation study in Au+Au collisions*, Rom.Rep.Phys. 58 (2006), 049-054, arXiv:nucl-ex/0510069